Food and Bioproducts Processing 155 (2026) 179–188

Contents lists available at ScienceDirect

Food and Bioproducts Processing

journal homepage: www.elsevier.com/locate/fbp

Enzymatic dispersion of pseudomonad biofilms grown at psychrotrophic temperature

Srinithi Muthuraman *, Jon Palmer, Steve Flint

Food microbiology, Biofilm research, School of Food Technology and Natural Science, Massey University, Palmerston North 4412, New Zealand

ARTICLE INFO

Keywords:
Pseudomonads
Psychrotrophic
Enzymes
Dispersion
Cellulose

ABSTRACT

Pseudomonads are robust biofilm formers in psychrotrophic temperatures, which can cause spoilage in dairy, poultry, and meat processing. This study screened eleven isolates for the biofilm-forming ability using the Congo Red Assay (CRA) and the crystal violet assay. Two isolates, 3SM and 20SM, showed significantly higher EPS production, cellulose synthesis and cell count at 4°C and were selected for the enzymatic dispersion. Mature biofilms formed on the stainless-steel surface for 72 h at 4°C were treated with laboratory enzymes (Proteinase-K, Cellulase, and DNase I) and commercial enzymes (formulated cleaners, EnduroZyme, DualZyme, and TriZyme). Compared to laboratory enzymes, commercial enzymes were efficient in dispersing the biofilms (EnduroZyme-62 %, DualZyme- 42 %, and TriZyme-32 % of biofilm removal), which was confirmed by cell counts, crystal violet assay, and microscopic observations. However, none of the treatments resulted in complete biofilm dispersion. These findings highlight the resilience of psychrotrophic pseudomonad biofilms and underscore the need for improved enzymatic strategies tailored for cold-chain environments.

1. Introduction

Pseudomonads are Gram-negative rods that produce a wide range of thermostable proteolytic and lipolytic enzymes responsible for spoilage in dairy, poultry, and meat processing environments (Weidmann et al., 2000; Parlapani et al.,2023). Biofilms of pseudomonads cause continuous contamination in the food processing environments (Raposo et al., 2016). Strong extracellular polymeric substances (EPS) and robust biofilm formation at cold temperatures are responsible for their spoilage potential in cold chain processing (Liu et al., 2023).

The cold stress, reduced motility, and the structural elements in the EPS matrix, such as polysaccharides including cellulose, curli fibres, proteins, lipids, and eDNA (Flemming & Wingender, 2010; Wickramasinghe et al., 2020). Cellulose and curli fibers have been identified in the biofilm formation of *Escherichia coli*, *Salmonella,* and some other proteobacteria (Wang et al., 2023; Abidi et al., 2022). Bacterial cellulose in biofilms is mainly seen in oxygen-dependent organisms that form strong biofilms at an air-liquid interface and is known for its high-water retention and mechanical strength (Mbituyimana et al., 2021).

Due to reduced diffusivity generated by the EPS, the biofilm can protect the bacterial cells from antimicrobials and cleaning chemicals (Aswath Narayan and Vittal, 2014). Studies even showed that biofilms are composed of 90 % EPS, mainly polysaccharides, and less than 10 % cells (Flemming et al., 2017). The EPS is composed of polysaccharides, proteins, lipids and eDNA (Flemming & Wingender, 2010). The complex EPS structures and interactions between the EPS components maintain the integrity of the biofilms. The traditional cleaning chemicals, such as NaOH, chlorine and acids, failed to remove the biofilms on the food contact surfaces. The clean-in-place involves thermal and non-biodegradable chemicals, leading to question about the sustainability of these processes (Pant et al.,2023). To overcome these limitations, there are studies focusing on environmentally friendly strategies to control these biofilms. Enzymes are among those strategies that can target the components of the EPS and disperse the biofilms and may play a critical role in biofilm removal (Pant et al.,2023; Nahar et al.,2018; Muthuraman et al.,2025b).

Enzymes are mainly proteins and can act as catalysts and accelerate the chemical reactions (Cooper, 2000). Enzymes target the polysaccharides, proteins and eDNA of the biofilm EPS matrix. The glycoside hydrolases, such as cellulase and α-amylases, target the β-1,4 linkages and α-1,4 linkages of glycosidic bonds and break down the polysaccharides in the EPS matrix (Kovach et al., 2020). The phosphor diester bonds of eDNA can be lysed by the DNase enzyme and which can disrupt the biofilms of *P. aeruginosa* (Kovach et al.,2020). DNase I is

* Corresponding author.
E-mail address: S.Muthuraman@massey.ac.nz (S. Muthuraman).

https://doi.org/10.1016/j.fbp.2025.12.015
Received 11 October 2025; Received in revised form 9 December 2025; Accepted 12 December 2025
Available online 13 December 2025

known to prevent the eDNA and EPS interactions and disperse the biofilms in the early stages. Proteins are the other major component of the biofilms, and there are various proteinaceous enzymes that can break down the proteins in the EPS matrix (Kumar Shukla & Rao, 2013).

The enzyme activity depends on various parameters. Studies focused on single enzymes adapted to the temperature of 37ºC and incubated for different time intervals (Nguyen and Burrows, 2014; Deng et al., 2022). While the commercial enzyme cleaners work at higher temperatures and with a combination of enzymes (Parkar et al., 2004; Tang et al., 2010; Puga et al.,2018). The DNase I and proteinase K against *Listeria monocytogenes* biofilms at 24 h dispersed the biofilms in a dose-dependent manner, explaining that the enzyme activity is strongly affected by temperature, enzyme doses, and the biofilm maturity (Nguyen and Burrows, 2014).

In our previous study, cellulose and polysaccharides were identified as major components of the EPS matrix of these pseudomonad isolates, followed by proteins and eDNA (Muthuraman et al.,2025a). This present study focused on targeting the major EPS components using cellulase, proteinase K, DNase I, and commercial enzyme formulations made up of amylase, proteinase and lipases at cold temperatures. The previous studies either focused on single enzymes or commercial formulations and on the biofilms grown at 30–37ºC and the advantages of enzyme cleaners over single enzymes. To address these gaps, this present study compared the single enzymes and commercial enzymes on the matured Pseudomonad biofilms grown at cold chain temperatures.

2. Materials and methods

2.1. Bacterial isolates and culture conditions

Eleven dairy isolates (1SM, 2SM, 3SM, 4SM, 5SM, 6SM, 7SM, 16SM, 20SM, 38SM, 44SM (identification of these bacterial species is listed in the supplementary file 1) were used in this study. All these isolates were obtained from raw milk collected from different dairy farms across New Zealand. Identifications were confirmed using PCR and 16S rRNA sequencing.

Fresh, overnight cultures were prepared by streaking a stock culture (stored at −80°C) on a TSA agar plate, incubating at 30°C, and inoculating a single colony in the Tryptic soy broth (TSB, Difco™, Becton, Dickinson and Company, USA) overnight at 30°C. This overnight culture (18 h) was used for further experiments. This overnight inoculum was 10-fold serially diluted in sterile saline and plated on TSA plates to standardize the inoculum containing approximately 5.5–6 log CFU/mL of cells.

2.2. Congo red assay (CRA)

Expression of extracellular cellulose and curli was evaluated using the Congo red assay reported by Cimdins and Simm (2017). Tryptone agar (10 g/L of tryptone and 15 g/L of agar) was chosen due to the transparency and low interference with the results. Aliquots of Congo Red (2 g/L) (Congo Red, Sigma-Aldrich, USA) and of Coomassie Brilliant Blue (1 g/L) (Coomassie Brilliant Blue G-250, Sigma-Aldrich, USA) were prepared as aqueous solutions and autoclaved (121°C for 15 min). The above-mentioned stains were added later to the autoclaved tryptone agar at 55°C.

Overnight cultures (18 h) were streaked onto the agar plates and incubated at 30°C for 24–120 h. The colony morphology in Table 3 was recorded at 72 h due to the stable phenotype observed. The colony colours indicate curli and cellulose (red), curli (brown), cellulose (pink), and none (white). According to Cimdins and Simm (2017), the dry and rough colonies indicate higher levels of cellulose or curli, and the smooth colonies indicate lower levels.

2.3. Cellulose production

Cellulose production was quantified using Anthrone colorimetry (Wang et al., 2023). The stock cultures of the isolates were streaked onto TSA plates and incubated at 30°C for 24 h and 48 h as triplicates. After incubation, approximately 3 g of wet-weight colonies were collected in a 15 mL centrifuge tube using a cell scrapper. The extraction solution, consisting of an 8:2:1 ratio of acetic acid, nitric acid, and water, was added to the centrifuge tube. The mixture was boiled for 30 min and centrifuged at 11880 *g* for 5 min. The supernatant was discarded, and the pellet was washed with 1 mL of water and 1 mL of acetone and left overnight for drying. The dried pellet was dissolved in 1 mL of H_2SO_4. Then 0.1 mL of the mixture was added to 0.5 mL of Anthrone (Anthrone ACS reagent, Sigma-Aldrich, USA) (0.2 g in 100 mL of H_2SO_4), and the absorbance was read at 620 nm. Microcrystalline cellulose (Cellulose, Sigma Aldrich, USA) solutions of 25 mg/mL, 50 mg/mL, and 100 mg/mL were used as standards. The cellulose production was expressed as mg/mL and the strong cellulose producers were identified (Wang et al., 2023).

2.4. Biofilm formation

The biofilms were allowed to grow on flat-bottom 96-well microtiter plates (FALCON®, Corning Incorporated, Durham, USA). A cell suspension (as described in Section 2.1) was diluted to obtain an OD_{600} (Absorbance at 600 nm) of 0.05 ± 0.0015 (Varioskan Lux 3020–1333, Thermo Fisher, USA) with half-strength TSB. Next, 200 µL of the diluted inoculum was added to the wells of a 96-well microtiter plate. Two hundred microliters of half-strength TSB were added as a control. The plates were incubated at 4°C for 24,48, and 72 h.

The strong biofilm-forming isolates 3SM and 20SM were chosen for the biofilm formation on stainless-steel surface and enzyme removal. The stainless-steel coupons (SS) used in this study were 2.4 cm× 2.4 cm and 1 mm in thickness (316 with 2B finish). The coupons were passivated (with 50 % nitric acid at 70°C for 30 mins) to clean and generate an oxide coat on the surface (as is practiced in the food industry to reduce the possibility of corrosion) before being used for the biofilm formation assay (Zhao et al., 2019). The SS coupons were sonicated for 15 min to remove the adhering cells and cleaned with ethanol (Absolute ethanol, Thermo Fisher Scientific, USA) and Tri Gene (Tri Gene, Tristel Solutions Ltd, UK) (composition listed in supplementary file 1). The cleaned coupons were allowed to dry overnight and autoclaved at 121°C for 15 min. The SS coupons were placed diagonally in the vials (Plastic vials, Techno Plas Ltd, Australia) and filled with 4 mL of the inoculum (OD_{600} of 0.05 ± 0.0015, approximately 6 log CFU/mL) to create an air-liquid interface on the surface of the coupons. The coupon-containing vials were incubated at 4°C for 72 h.

2.5. Crystal violet assay

After the required incubation time, the microtiter plates were inverted to remove the liquid contents in the wells. The wells were washed three times with sterile distilled water to remove all the planktonic and loosely attached cells and allowed to dry for 30 min. Two hundred microliters of 0.5 % crystal violet (CV) (Crystal violet stain, Sigma-Aldrich, USA) were added to each well. After 15 min, the crystal violet-containing wells were washed three times with sterile distilled water, then allowed to dry for 30 min. Next, 230 µL of 96 % ethanol was added to the wells to dissolve the absorbed crystal violet and allowed to stand for 15 min. After 15 min, the absorbance of the ethanol solution was read at 570 nm.

After the required incubation time, the SS coupons were taken out and washed three times with sterile distilled water and allowed to air-dry for 30 min. The dried coupons were added to the 6-well microtiter plates (FALCON®, Corning Incorporated, Durham, USA) filled with 4 mL of 0.5 % crystal violet. After 15 min, the coupons were taken out

and washed three times with sterile distilled water and allowed to air-dry for 30 min. The stained coupons were added to the 6-well plates containing 4 mL of 96 % ethanol for 15 min. The contents were transferred to the 96-well plates and read at 570 nm.

Based on the CV values, the isolates were classified as strong, weak, and moderate biofilm formers based on the following criteria described by Xu et al. (2016) (Table 1).

2.6. Quantification of biofilm cells

After the required incubation period, the wells of the PS microtiter plates were washed three times with sterile distilled water. Then, using sterile cotton swabs (CITOSWAB®, Wellkang Ltd, Northern Ireland), the wells were swabbed and swirled in 1 mL of sterile saline (0.85 %). Then, 100 µL of the samples were serially diluted, and 10 µL of the drops were plated on TSA plates. The numbers of cells present in the wells (surface area 0.32 cm^2) were expressed as log CFU/cm^2.

After required incubation, the coupons were taken out and washed three times with sterile distilled water. The coupons were swabbed using sterile cotton swabs and swirled in 1 mL sterile saline (0.85 %). Then, 100 µL of the samples were serially diluted, and 10 µL of the drops were plated on TSA plates. The numbers of cells present in the coupons (surface area 2.88 cm^2) were expressed as log CFU/cm^2.

2.7. Treating the preformed biofilms with Laboratory enzymes

Biofilms were allowed to form on the stainless-steel coupons for 72 h. A total of 10 technical replicate coupons were used for each biological replicate (crystal violet assay-3, cell counts-3, and microscopic observations 3). Cellulase (Cellulase from *Aspergillus niger*, Sigma Aldrich Inc., USA), Proteinase-K (Proteinase-K, Recombinant, Sigma Aldrich Inc., USA), and DNase I (DNase I from bovine pancreas, Sigma Aldrich Inc., USA) were used in this study to understand the effects of enzymes on preformed biofilms. Proteinase K and cellulase stock and working solutions were prepared in sterile distilled water. The DNase I stock solution was prepared by diluting in sterile distilled water, and the working solution was prepared in phosphate buffer saline (PBS, Thermofisher Scientific, USA) containing 5 mM of Mg^{2+}. All the enzymes were tested in 10, 100, and 200 µg/ mL concentrations. After 72 h of incubation, the coupons containing the vials were removed from the incubator. The coupons were transferred to the vials containing 5 mL of enzymes and kept at 37°C for an hour. The coupons were stained with crystal violet to determine the biomass, and the coupons were swabbed, serially diluted, and plated to determine the cell counts after treatment with enzymes (Nguyen & Burrows, 2014).

2.8. Commercial enzyme cleaners

The commercial enzymes from IXOM (IXOM, Australia) were used to treat the preformed biofilms as per the manufacturer's instructions (Table 2).

The coupons were taken out after 72 h of incubation and washed in sterile distilled water. The washed coupons were added to the vials containing 5 mL of commercial enzyme cleaner solutions. The vials were incubated at 50°C for an hour. Cell counts and OD_{570} were recorded. The optimum temperatures for both laboratory and commercial enzymes were used per the manufacturer's recommendations.

Table 1
Classification of biofilm formation based on crystal violet assay (Xu et al.,2016).

No biofilm formation	$OD_{570} < OD_{570con}$
Weak biofilm formation	$OD_{570con} < OD_{570} \leq 2\ OD_{570con}$
Moderate biofilm formation	$2OD_{570con} < OD_{570} \leq 4\ OD_{570con}$
Strong biofilm formation	$4\ OD_{570con} \leq OD_{570}$

*OD_{570con} – OD_{570} values from control wells with no biofilm formation
*OD_{570} . OD_{570} values from the wells with biofilms

Table 2
The commercial enzymes used in this study.

Product	Composition	Temperature	Concentration	pH
Superflux EnduroZyme	Protease	50°C	0.5 % v/v	11
Superflux Dual Zyme	Protease and Lipase			10
Superflux Tri Zyme	Protease, cellulase, and amylase			10

2.9. Microscopical observations

Acridine orange was used to check the dispersion of cells from the biofilms. The control (untreated coupons with biofilms on the surface) and treated coupons (coupons with biofilms treated with enzymes and enzyme cleaners) were washed with sterile distilled water and allowed to air dry. One hundred microlitres (100 µL) of the stains were added to the coupon surface for 3 min. The coupons were washed and dried. The dried coupons were observed under an epifluorescence microscope (Nikon Eclipse Ni-L, Nikon Instruments, USA) with a suitable filter TRITC (Excitation 532–550 nm and emission 574 nm) for acridine orange. The images were captured with NIS-elements D software (Version 6.02.01(Build 1955), Nikon Instruments, USA).

2.10. Data analysis

The means and standard deviation (SD) for cell counts and OD_{570} values were based on three biological and three technical replicates. One-way analysis of variance (ANOVA) with a Tukey's test with a *p*-value below 0.05 indicated the significance of the results. analysis was conducted using SPSS software (Version 29.0.2.0; IBM®, New York, United States).

3. Results

3.1. Congo red assay (CRA)

The CRA plates were observed from 24 h to 120 h. Different colony

Table 3
Colony morphology observed with Congo Red Assay.

Isolates	Colony morphology	Indication	Biofilm formation
1SM	Brown, dry, and rough colonies (*Bdar*)	Curli-only producer, impaired cellulose production	Strong
2SM	Red and smooth colonies	Low levels of cellulose and curli	weak
3SM	Pink, dry, and rough colonies (*Pdar*)	Cellulose only producer and impairment of curli.	Strong
4SM	Red and smooth colonies	Low levels of cellulose and curli	Weak
5SM	Red, dry, and rough colonies (*Rdar*)	Production of both cellulose and curli	Strong
6SM	Blue, dry, and rough colonies	Levan	-
7SM	Red and smooth colonies	Low levels of cellulose and curli	Weak
16SM	Red and smooth colonies	Low levels of cellulose and curli	Weak
20SM	Pink, dry, and rough colonies (Pdar)	Cellulose only producer and Impairment of curli.	Strong
38SM	Brown and smooth colonies	Low levels of curli and impairment of Cellulose.	Weak
44SM	White, smooth colonies	Neither cellulose nor curli	Weak

morphologies were observed (Table 3). The pink, dry, and rough *(Pdar)* (Fig. 1 A) colonies indicate the production of cellulose only, the brown, dry, and rough *(Bdar)* (Fig. 1B) colonies indicate the production of curli only, while the red, dry, and rough *(Rdar)* (Fig. 1E) colonies indicate the production of both cellulose and curli. The white and smooth colonies (Fig. 1 C) indicate the production of neither curli nor cellulose. The blue colonies (Fig. 1D) indicate the Levan production (supplementary file 2).

3.2. Quantification of cellulose

The amount of cellulose produced by isolates correlated with the results from the Congo Red Assay. The following isolates, 1SM, 6SM, 38SM, and 44SM, did not produce cellulosic colonies on CRA and showed zero OD_{620} with Anthrone colorimetry. The low cellulose producers indicated by CRA were 2SM, 4SM, 7SM, and 16SM produced cellulose between 3.71 and 4 mg/mL of cellulose (Fig. 2). The cellulose-only producers 3SM, 20SM, and cellulose and curli producer 5SM showed high amounts of cellulose among the 11 isolates.

3.3. Biofilm formation

The screening of the strong biofilm formers based on crystal violet assay and cell counts resulted in two strong biofilm formers, 3SM and 20SM (Fig. 3 A and 3B). Both isolates showed significantly ($p < 0.05$) higher OD_{570} values, 3.188 ± 0.37 (3SM) and 3.21 ± 0.41 (20SM), compared to other isolates. These isolates showed significantly ($p < 0.05$) higher cell counts, which were 7.52 ± 0.13 (3SM) and 7.59 ± 0.18 log CFU/cm^2 (20SM). Other isolates formed weak biofilms with half-strength TSB at 4°C.

3.4. Effects of cellulase, DNase I, and Proteinase-K on the preformed biofilms

Proteinase-K 10–200 µg/mL failed to disperse the biofilms

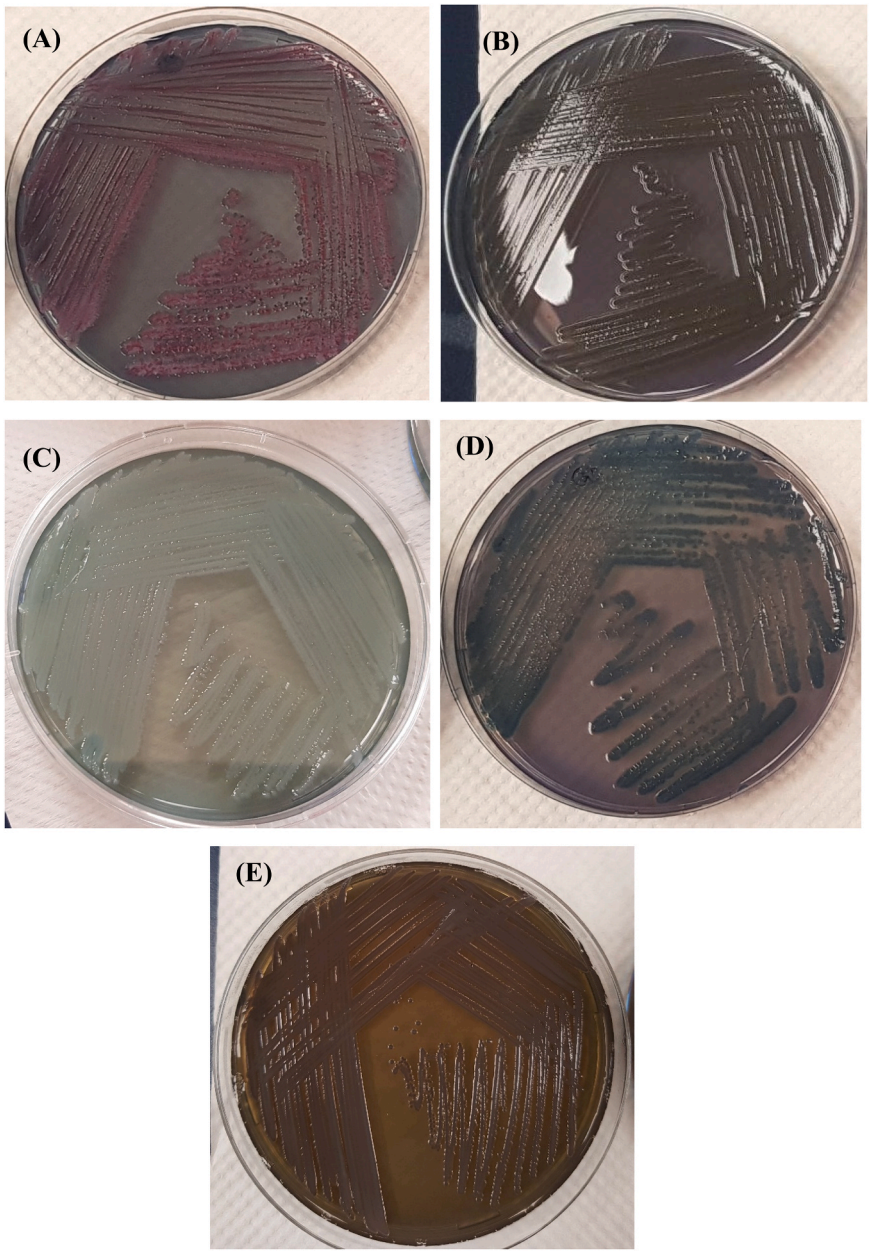

Fig. 1. (A) Pink, dry, and rough colonies (*Pdar*, Isolate 3SM), (B) Brown, dry, and rough colonies (*Bdar*, Isolate 1SM), White and smooth colonies (44SM), (D) Blue coloured colonies (Isolate 6SM), (E) Red, dry and rough colonies (*Rdar* 5SM).

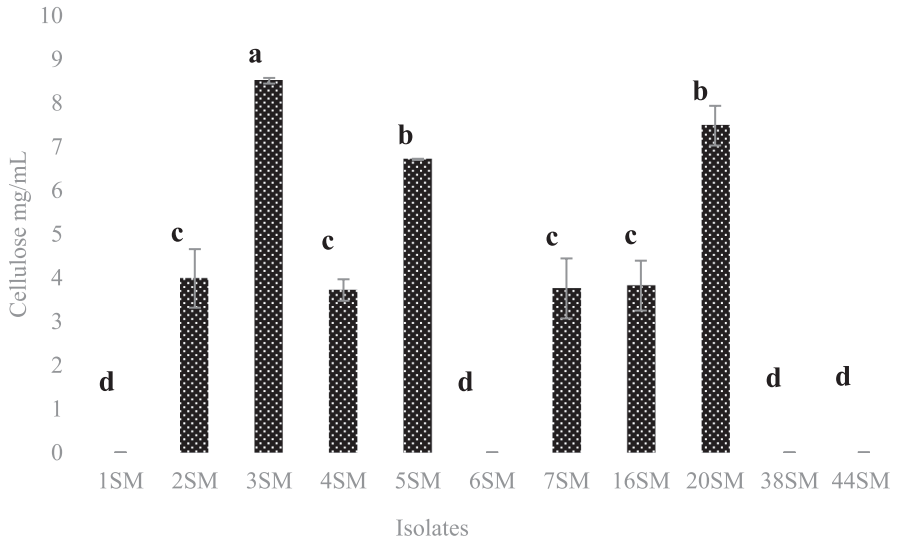

Fig. 2. Cellulose produced by different isolates of pseudomonads, different letters above the bars indicate significant differences ($p < 0.05$).

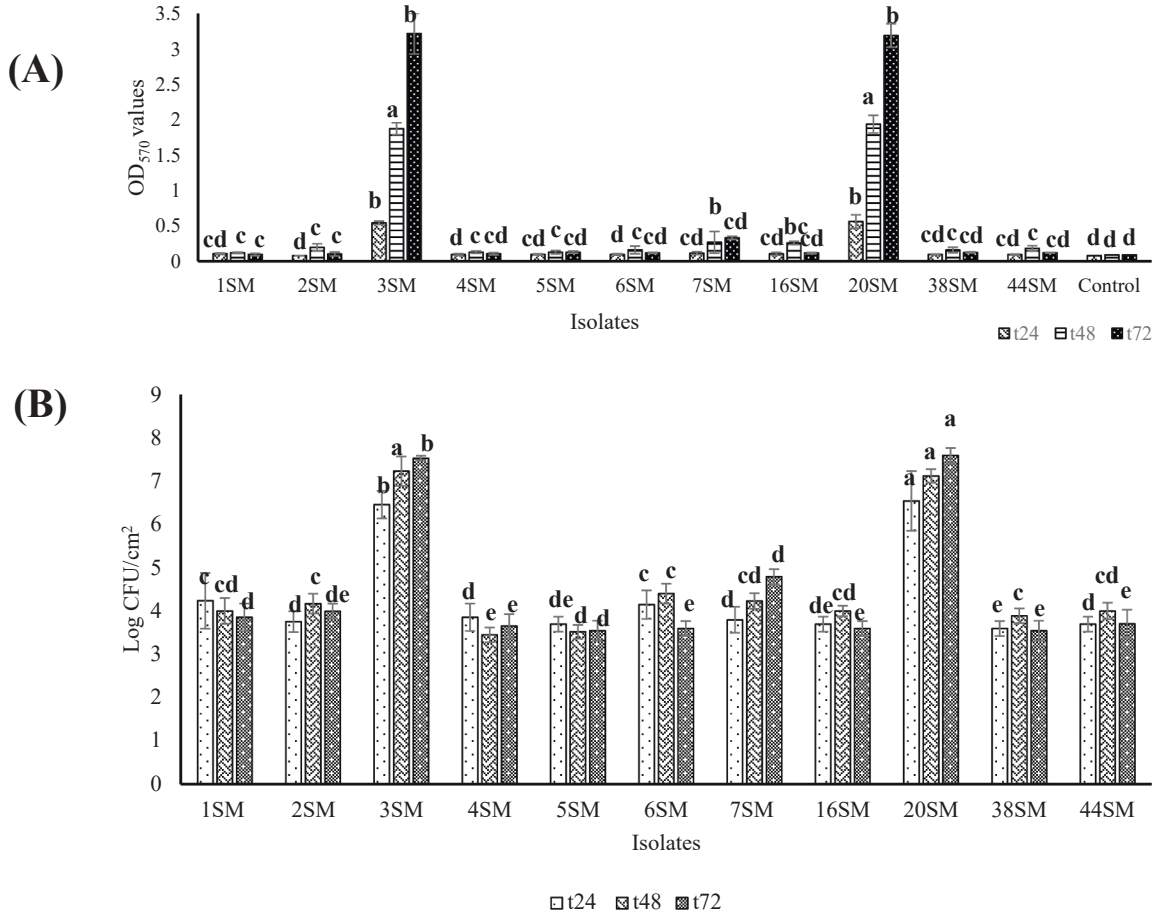

Fig. 3. (A) OD_{570} values from the crystal violet assay at 4°C with half-strength TSB and (B) the cell counts at 4°C with half-strength TSB. All the results are expressed as mean ± standard deviation. Different letters above the bars indicate significant differences ($p < 0.05$).

completely. The CV values after treating with 10 μg/mL of proteinase-K, resulting in 2.58 ± 0.11 (3SM) and 2.49 ± 0.05 (20SM) (Fig. 4A), were almost the same as the untreated control coupons. However, with 100 and 200 μg/mL, there was a slight decrease in the CV values observed when compared to the control coupons. Overall, proteinase-K did not completely remove the EPS of these psychrotrophic pseudomonads. With higher concentrations such as 100 and 200 μg/mL, the reduction in the cell counts was 0.65 ± 0.09 log CFU/cm^2 (Fig. 4B). The lower concentration of Proteinase-K, 10 μg/mL, showed similar cell counts as the control coupons, indicating there was no effect.

For isolate 3SM, 200 μg/mL of DNase I enzyme removed 0.5 log CFU/cm^2 of cells compared to the control coupons (Fig. 4B). While for

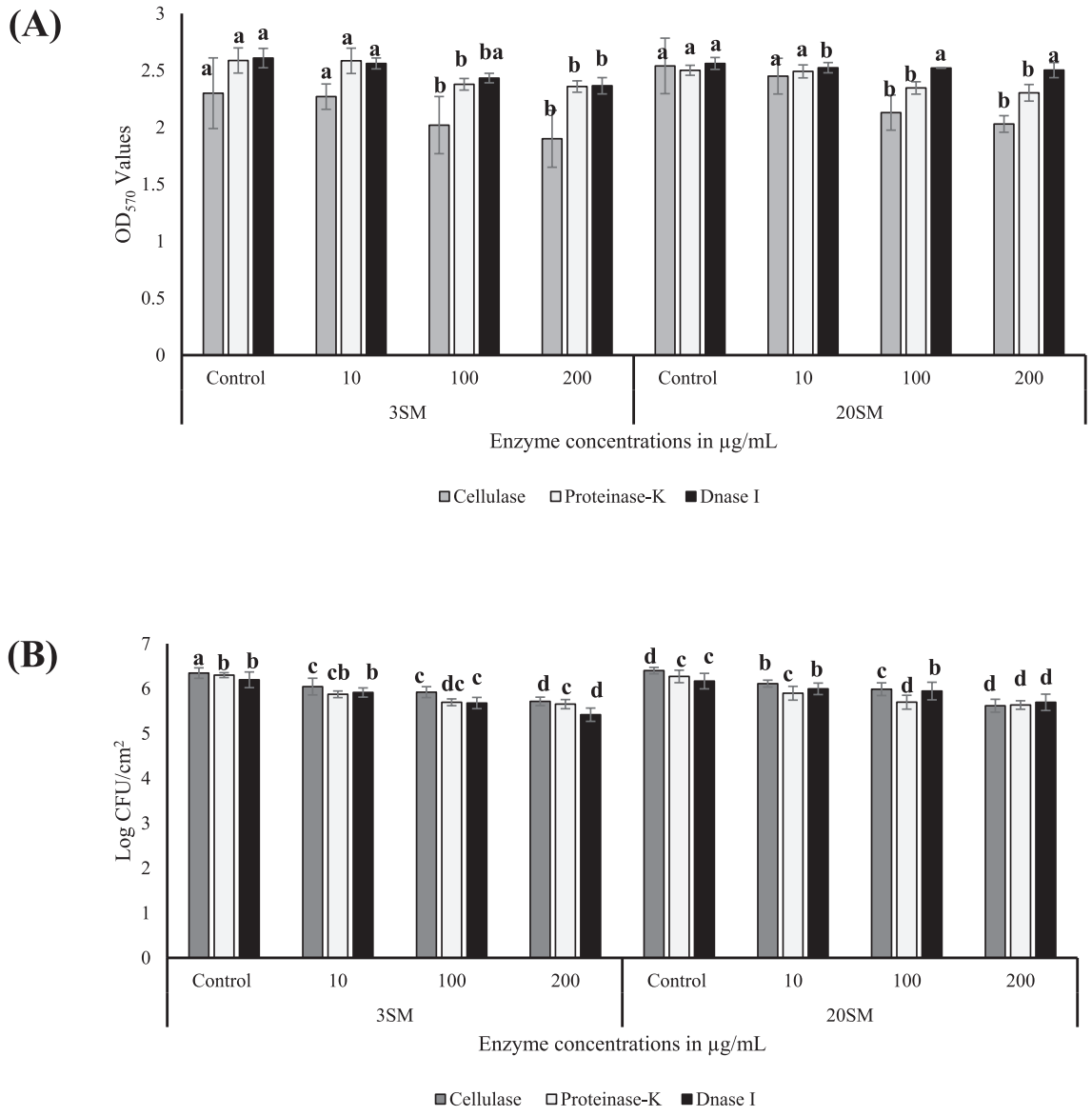

Fig. 4. Graph (A) shows the crystal violet values of strong biofilms when treated with enzymes, while Graph (B) shows the cell counts of the strong biofilm formers 3SM and 20SM after being treated with enzymes. All the results are expressed as mean±standard deviation. Different letters above the bars indicate significant differences ($p < 0.05$).

the isolate 20SM, the cell count difference was around 0.4 ± 0.08 log CFU/cm^2. The OD_{570} values were significantly ($p < 0.05$) lower for the preformed biofilms of isolate 3SM when 200 µg/ mL of DNase enzyme was added for an hour at 37°C was 2.35 ± 0.33 (Fig. 4A). However, it was not even a log reduction, and the dispersion of the biofilms was not observed.

There were about 0.6–0.8 log CFU/cm^2 (Fig. 4B) reductions in the cell counts observed for isolates 3SM and 20SM after treatment with cellulase at 200 µg/mL. When the biofilms were treated with 10 and 100 µg/mL, the cell reductions were between 0.4 and 0.3 log CFU/cm^2 observed for the isolates 3SM and 20SM. Even though there was a significant ($p < 0.05$) difference between the control and treated biofilm samples, cellulase failed to completely disperse the biofilms.

3.5. Commercial enzyme cleaners

Compared to the other enzymes, the commercial enzymes were effective in biofilm dispersion. The EnduroZyme significantly ($p < 0.05$) dispersed the pseudomonad biofilms compared to the TriZyme and DualZyme with the crystal violet assay and cell counts. DualZyme and TriZyme removed 1.37 and 1.95 log CFU/cm^2 (Fig. 5B) cells from the preformed biofilms of isolates 3SM and 20SM, whereas the log reduction for EnduroZyme was 2.21 and 3.38 log CFU/cm^2. Compared to cellulase, proteinase-K, and DNase I, the commercial enzymes showed a significant ($p < 0.05$) reduction in the OD_{570} values (Fig. 5A). However, the complete dispersion or removal was not achieved with commercial enzymes.

3.6. Microscopic observations

The eDNA channels formed on the biofilm surface were present in all the samples, even those treated with enzymes (Fig. 6). The DNase I enzyme, known for degrading eDNA, could not remove the eDNA channels. The biofilms treated with higher concentrations of enzymes showed the aggregates (Figs. 6A and 6B) and the stainless-steel surface, while the control and 100 µg/mL enzyme-treated coupons showed biofilm cells completely covering the surface. This indicates that the enzymes could target the biofilm matrix. These structural changes in

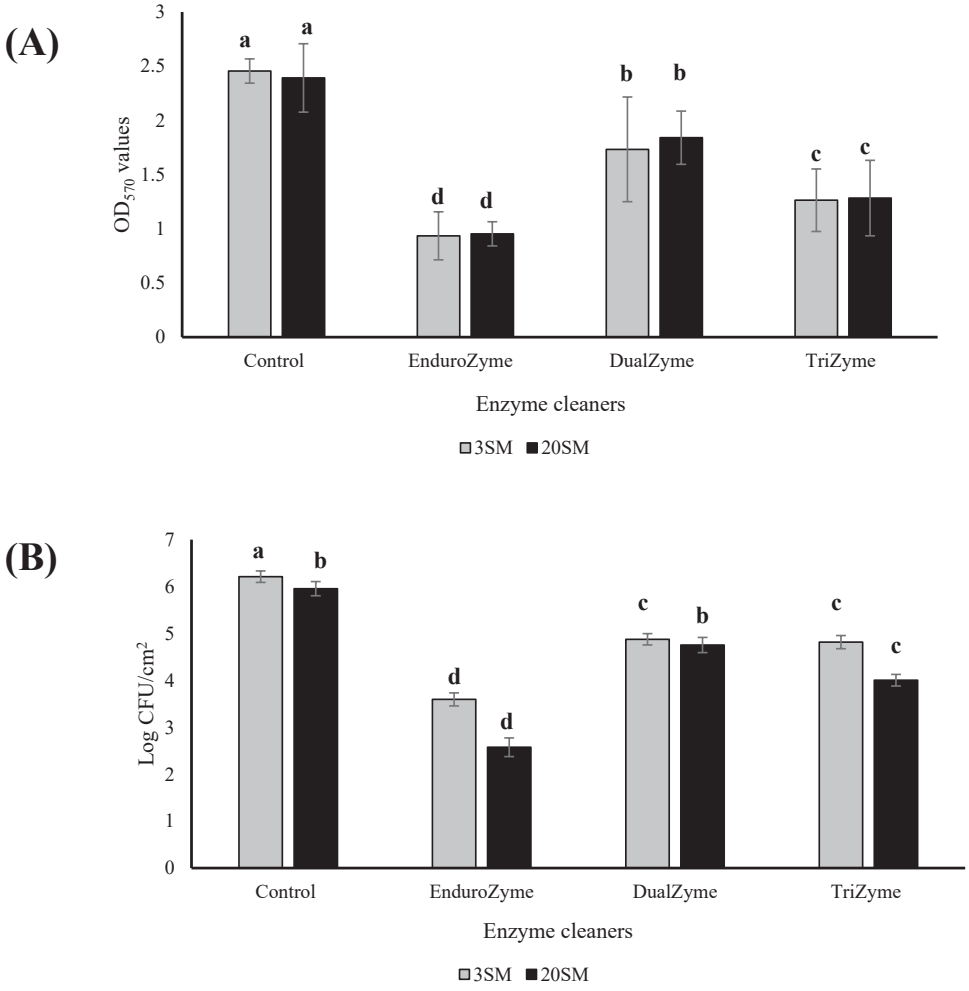

Fig. 5. Graph (A) Crystal violet values of strong biofilms treated with commercial enzyme cleaners, while graph (B) shows the cell counts of the strong biofilms 3SM and 20SM treated with commercial enzyme cleaners. All the results are expressed as mean±standard deviation. Different letters above the bars indicate significant differences ($p < 0.05$).

microscopic observations support the cell counts and crystal violet biomass values, suggesting minimal biofilm reduction rather than partial or complete removal.

Similar trends were observed in the biofilm removal by commercial enzyme cleaners. Compared to the control coupons (Fig. 7A), the coupons treated with EnduroZyme showed clear differences in dispersion of the biofilms (Fig. 7B). The reduction in cell counts and biofilm biomass can be clearly seen with the microscopic observations. The coupons treated with DualZyme and TriZyme (Fig. 7C & 7D) did not differ much from the control coupons, and the cell counts and crystal violet data showed similar results. Even though the EnduroZyme was strong enough to disperse the biofilms, the eDNA and Psl network can still be seen (Fig. 7E). Even with commercial enzymes, the pseudomonad biofilms cannot be completely dispersed.

4. Discussion

Different morphotypes were identified from the CRA in this study: (1) curli-only producers, (2) cellulose-only producers, (3) curli and cellulose producers, and (4) neither cellulose nor curli producers. In this present study, the strong biofilm formers are cellulose-only producers (*Pdar* morphotype), and the absence of curli fibres did not affect their biofilm formation, while the *Bdar* (1SM) and *Rdar* (5SM) failed to form strong biofilms. In *Salmonella* Typhimurium and *E. coli,* the co-production of cellulose and curli fibers results in a strong hydrophobic extracellular polymeric substance matrix. In contrast, either cellulose or curli production results in a fragile matrix (Flemming & Wingender, 2010). A study with curli and cellulose genes of *E. coli* MG1655 showed cellulose provides resistance to environmental stress rather than simply biofilm formation (Gualdi et al., 2008). The divergent ability of *Bdar* and *Rdar* to produce cellulose leads to biofilm development and resistance of *S.* Typhimurium biofilms (Kim et al., 2022). The results from the Congo Red Assay did not reflect the biofilm formation of all the isolates tested in this study.

The curli only producers 1SM and 38SM, Levan producer 6SM, and no curli and cellulose producer 44SM did not produce the brown colour, which is an indication of cellulose production with Anthrone colorimetry. These results agreed with the CRA. *Pdar* and *Rdar* morphotype isolates 3SM and 20SM showed a higher amount of cellulose than the rest. The cellulose production by *Bdar* and *Pdar* morphotypes of *Vibrio parahaemolyticus* revealed that pink colony formers produced cellulose, while there was no cellulose produced by the brown morphotypes (Wang et al., 2023). The brown morphotypes were also weak biofilm formers in that study. This present study showed similar results in that the brown morphotype was a weak biofilm former, and the pink morphotypes were the strong biofilm formers. However, the reason behind the weak biofilm formation of another cellulose producer, 5SM, is not well known, and the cellulose production only correlated with the strong biofilm formers.

In this present study, the cellulose producers identified from CRA

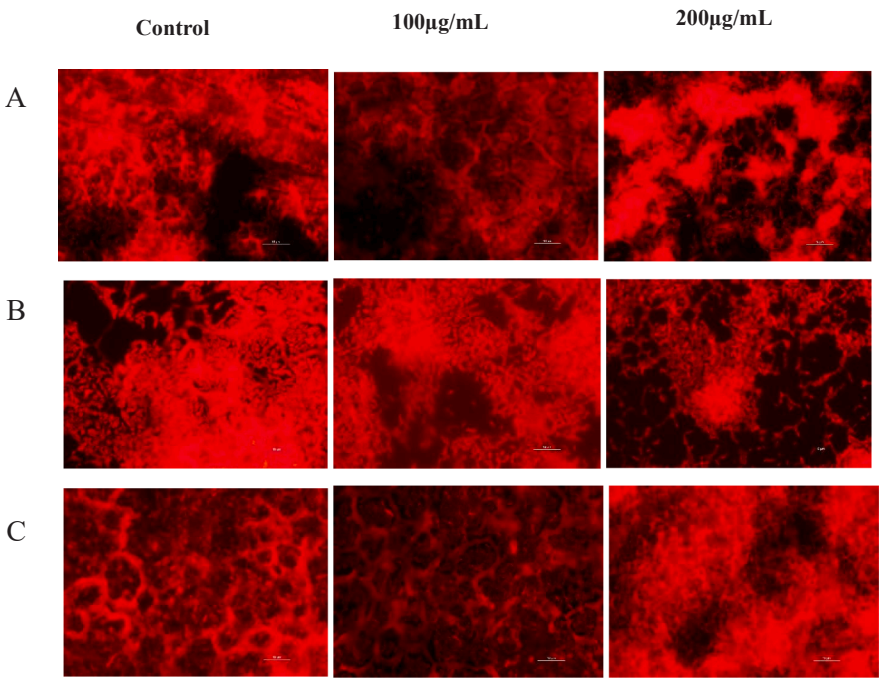

Fig. 6. Epifluorescence microscopic images of pseudomonad biofilms stained with acridine orange (binds with nucleic acids and stains the live cells) (A) Biofilms formed by isolate 3SM treated with Proteinase-K, (B) treated with DNase I, (C) treated with cellulase (Scale bar 10 µm).

formed strong biofilms at the air-liquid interface. However, the air-liquid interface did not encourage the biofilm formation of weak biofilm formers. This suggests that cellulose production is important in the formation of robust biofilms of psychrotrophic pseudomonads. However, the weak biofilm formation of *Rdar* morphotype 5SM did not correlate with cellulose production and biofilm formation. In a report by Ardré et al. (2019) on *P. fluorescens* SBW25, the cellulose production at the air-liquid interface is mediated via wrinkly spreaders (Wps), the air-water-surface (Aws), and the micro-water-surface (Mws) known as diguanylate cyclase-encoding pathways. The environmental signals at the air-liquid interface trigger cellulose production and robust biofilm formation via these three pathways.

In this present study, among the 11 isolates, two of them (3SM and 20SM) could form strong biofilms at 4ºC. These two isolates were chosen for further study based on their biofilm biomass, cellulose production and thick visible biofilms at the air-liquid interface. However, the link between cellulose production and robust biofilm formation at cold temperatures needs to be studied. *P. lundensis* from a meat source was reported to form higher biofilms and higher cell counts at 10 and 4°C compared with 25°C (Liu et al., 2015). Pseudomonads grown on meat surfaces form stronger biofilms at cold temperatures compared to ambient temperatures due to the response to cold stress (Wickramasinghe et al., 2019). This present study also confirmed that cold temperatures encourage the biofilm formation of psychrotrophic pseudomonads.

In this present study, Proteinase K, Cellulase, and DNase I were used to disperse the biofilms. However, none of them could disperse the biofilms formed by pseudomonads even at concentrations of 200 µg/mL. When the *Listeria monocytogenes* biofilms were treated with proteinase-K, even the lower concentrations of proteinase-K down to 6.3 µg/mL at 37°C for an hour could completely disperse the biofilms. (Nguyen & Burrows, 2014). Eladawy et al., (2020) also observed no significant reduction in the biomass of *P. aeruginosa* preformed biofilms observed after treatment with proteinase-K. *Listeria monocytogenes* had higher proteins and lower polysaccharides in the EPS matrix (Puga et al.,2018), and their dispersion by proteinase was possible. The pseudomonads in this study had higher polysaccharides in their matrix. However, the failure of cellulase to disperse these biofilms was not clear.

In this present study, with DNase I, the cell biomass reduction was less than a log CFU/cm^2. When the biofilms of *L. monocytogenes* were treated with DNase I, similar reductions in the biomass were observed from the concentrations 6.3–200 µg/mL (Nguyen & Burrows, 2014). When the DNase I enzyme was immobilised with Ag nanoparticles, the biofilm started dispersing, and the viability of the *P. aeruginosa* cells was decreased. The microscopic observations showed fewer cells on DNase I and AgNP-treated biofilms. The cell reduction is because of silver rather than enzymes, indicating the ineffectiveness of enzymes. (Rubio-Canalejas et al., 2022). The eDNA was the third major component in the biofilm EPS of 3SM and 20SM (Muthuraman et al.,2025), and could be the reason for the ineffectiveness of DNase I. However, DNase I with the addition of Mg^{2+} (10 mM) could disperse around 80 % of the *P. aeruginosa* PAO1 preformed biofilms (Sharma & Pagedar Singh, 2018). The biofilms formed in the above-mentioned studies are not at cold temperatures. The robust EPS production at cold temperatures in this study and complex biofilm structures could contribute to the failure of enzymes to disperse these biofilms.

Compared to the laboratory enzymes, the commercial enzymes showed more than a log CFU/cm^2 in the biofilm removal of these pseudomonads in the present study. Subtilisin is the protease present in the commercial enzyme cleaner EnduroZyme, which was effective in the dispersion of the preformed biofilms in this study. Subtilisin A reduced the biofilm biomass of 24h-old *Staphylococcus aureus* biofilms and prevented the same isolate's biofilm formation (Liu et al., 2021). However, the biofilms in the present study were mature pseudomonad biofilms and strong EPS producers. The TriZyme and DualZyme in this study consist of a combination of enzymes, but the biofilm reduction was not higher than subtilisin alone. QuatroZyme is a combination of protease, lipase, amylase, and cellulase, which showed 6.15 and 5.31 log CFU/cm^2 reduction when treated on the single and dual strain biofilms of *Klebsiella oxytoca* (Tang et al., 2010). However, the highest cell reduction observed in the present study was 3.38 log CFU/cm^{2,} indicating the effects of enzyme cleaners differ based on the formulations and are highly dependent on the biofilm structure and composition.

There were notable differences between the laboratory enzymes and commercial enzyme cleaners. First, the laboratory enzymes were of single enzyme formulations, while the commercial enzyme cleaners

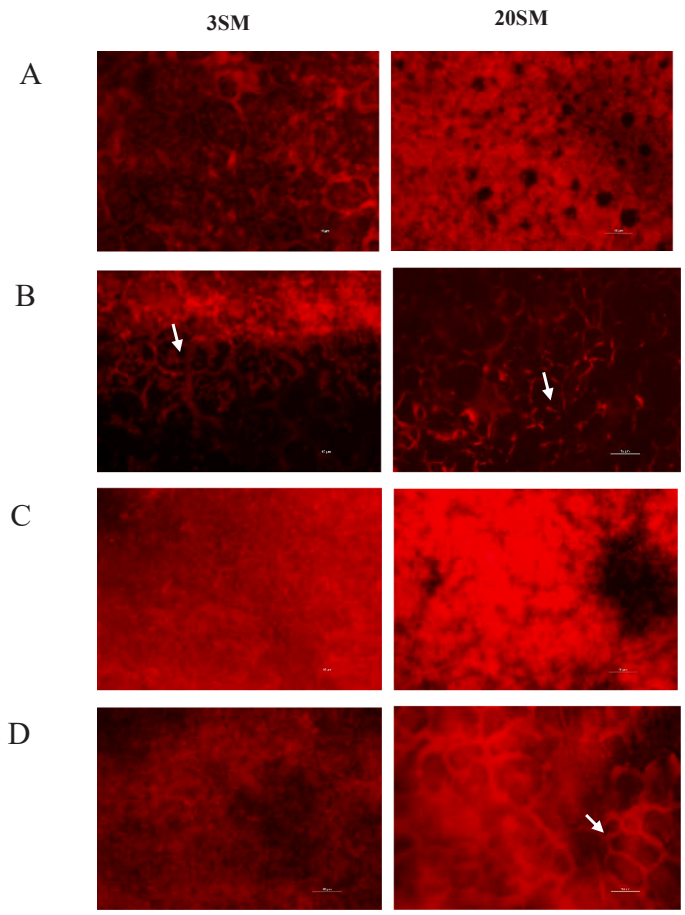

Fig. 7. Epifluorescence microscopic images of pseudomonad biofilms stained with acridine orange (binds with nucleic acids and stains the live cells). (A) control coupons, (B) treated with EnduroZyme, (C) treated with DualZyme, (D) treated with TriZyme (Scale bar 10 μm). White arrows show the eDNA and *Psl* network.

consist of single or more than two enzymes. Another key difference is the addition of stabilizers and biosurfactants in the commercial formulations. Thus, the performance of commercial enzyme cleaners was higher than that of laboratory enzymes. A limitation of this present study is that a single temperature could not be applied across all the enzyme treatments. Laboratory enzymes exhibit optimal activity at 37°C, while the commercial enzyme cleaners are formulated to perform at higher temperatures (50°C). This discrepancy may affect the direct comparisons and should be considered while interpreting differences between enzyme treatments.

In this present study, cellulase, proteinase, and DNase I failed to disperse the biofilms, and the eDNA and Psl network remained the same after treatment with enzymes, including the commercial enzyme cleaners. The microscopic observations showed the eDNA-Psl network even after cleaning with commercial enzyme cleaners (Fig. 7E). These results suggest the molecular interactions in the EPS matrix need to be considered for designing the elimination strategies. The eDNA and Psl network cannot be dispersed by the DNase I enzyme due to the complex limiting access of agents targeting only one substance (Wang et al., 2015).

Overall, this present study showed that pseudomonad biofilms in the cold chain environment are hard to clean, with both laboratory and commercial enzyme cleaners to achieve minimal to partial biofilm disruption. The limited reduction in cell counts and crystal violet values was comparable with the microscopic observations. The complex biofilm structures, such as eDNA and the Psl network, contribute to the robust nature of pseudomonad biofilms. The enzyme cleaners are promising strategies, as the commercial enzymes in this study could remove the biofilms by 68 % (EnduroZyme). Enzyme immobilisation can reduce particle size, increase zeta potential, and enhance enzyme penetrability (Rubio-Canalejas et al., 2022). Enzyme immobilization techniques could improve the efficiency of these commercial enzymes. Combining other strategies, such as sanitizers, biosurfactants, ultrasound, could improve the biofilm removal when combined with enzymes (Yuan et al., 2021). In summary, the results of this study emphasise the need to develop robust biofilm control strategies to tackle these biofilms at refrigeration temperatures.

5. Conclusion

The pseudomonad isolates in this study formed robust biofilms at cold temperatures. The findings in this study indicate that single enzymes are insufficient in eliminating these highly resilient biofilms. The commercial enzyme formulations showed promising results. However, this study highlights the need for improved strategies in eradicating pseudomonad biofilms at cold temperatures. Further studies are required to develop enhanced formulations, combine synergistic approaches, such as biosurfactants, sanitizers, and other mechanical and chemical treatments, to control these cold chain biofilms.

CRediT authorship contribution statement

Srinithi Muthuraman: Writing – review & editing, Writing – original draft, Methodology, Formal analysis, Conceptualization. **Jon Palmer:** Writing – review & editing, Supervision, Conceptualization. **Steve Flint:** Writing – review & editing, Supervision, Conceptualization.

Declaration of Competing Interest

The authors declare that they have no known competing financial interests or personal relationships that could have appeared to influence the work reported in this paper.

Appendix A. Supporting information

Supplementary data associated with this article can be found in the online version at doi:10.1016/j.fbp.2025.12.015.

References

Abidi, W., Torres-Sánchez, L., Siroy, A., Krasteva, P.V., 2022. Weaving of bacterial cellulose by the Bcs secretion systems. FEMS Microbiol. Rev. 46 (2), fuab051. https://doi.org/10.1093/femsre/fuab05.

Aswath Narayan, J.B., Vittal, R.R., 2014. Attachment and biofilm formation of *Pseudomonas fluorescens* PSD4 isolated from a dairy processing line. Food Sci. Biotechnol. 23 (6), 1903–1910. https://doi.org/10.1007/s10068-014-0260-8.

Cimdins, A., Simm, R., 2017. Semiquantitative Analysis of the Red, Dry, and Rough Colony Morphology of Salmonella enterica Serovar Typhimurium and Escherichia coli Using Congo Red. Methods Mol. Biol. (Clifton N. J.) 1657, 225–241. https://doi.org/10.1007/978-1-4939-7240-1_18.

Cooper, G.M., 2000. The chemistry of cells: The central role of enzymes as biological catalysts. In: Cooper, G.M. (Ed.), The cell: A molecular approach, 2nd ed., pp. 145–146.

Eladawy, M., El-Mowafy, M., El-Sokkary, M.M.A., Barwa, R., 2020. Effects of Lysozyme, Proteinase K, and Cephalosporins on Biofilm Formation by Clinical Isolates of *Pseudomonas aeruginosa*. Interdiscip. Perspect. Infect. Dis. 2020, 1–9. https://doi.org/10.1155/2020/6156720.

Fleming, D., Chahin, L., Rumbaugh, K., 2017. Glycoside hydrolases degrade polymicrobial bacterial biofilms in wounds. Antimicrob. Agents Chemother. 61 (2), 10–1128.

Flemming, H.-C., Wingender, J., 2010. The biofilm matrix. Nat. Rev. Microbiol. 8 (9), 623–633. https://doi.org/10.1038/nrmicro2415.

Gualdi, L., Tagliabue, L., Bertagnoli, S., Ieranò, T., De Castro, C., Landini, P., 2008. Cellulose modulates biofilm formation by counteracting curli-mediated colonization of solid surfaces in Escherichia coli. Microbiology 154 (7), 2017–2024. https://doi.org/10.1099/mic.0.2008/018093-0.

Kim, S.-H., Jyung, S., Kang, D.-H., 2022. Comparative study of Salmonella Typhimurium biofilms and their resistance depending on cellulose secretion and maturation temperatures. LWT 154, 112700.
Kovach, K.N., Fleming, D., Wells, M.J., Rumbaugh, K.P., Gordon, V.D., 2020. Specific Disruption of Established *Pseudomonas aeruginosa* Biofilms Using Polymer-Attacking Enzymes. Langmuir 36 (6), 1585–1595. https://doi.org/10.1021/acs.langmuir.9b02188.
Kumar Shukla, S., Rao, T.S., 2013. Dispersal of Bap-mediated Staphylococcus aureus biofilm by proteinase K. J. Antibiot. 66 (2), 55–60. https://doi.org/10.1038/ja.2012.98.
Liu, J., Madec, J.-Y., Bousquet-Mélou, A., Haenni, M., Ferran, A.A., 2021. Destruction of Staphylococcus aureus biofilms by combining an antibiotic with subtilisin A or calcium gluconate. Sci. Rep. 11 (1), 6225. https://doi.org/10.1038/s41598-021-85722-4.
Liu, J., Wu, S., Feng, L., Wu, Y., Zhu, J., 2023. Extracellular matrix affects mature biofilm and stress resistance of psychrotrophic spoilage Pseudomonas at cold temperature. Food Microbiol. 112, 104214. https://doi.org/10.1016/j.fm.2023.104214.
Liu, Y., Xie, J., Zhao, L., Qian, Y., Zhao, Y., Liu, X., 2015. Biofilm formation characteristics of *Pseudomonas lundensis* isolated from Meat. J. Food Sci. 80 (12).
Mbituyimana, B., Liu, L., Ye, W., Ode Boni, B.O., Zhang, K., Chen, J., Thomas, S., Vasilievich, R.V., Shi, Z., Yang, G., 2021. Bacterial cellulose-based composites for biomedical and cosmetic applications: Research progress and existing products. Carbohydr. Polym. 273, 118565. https://doi.org/10.1016/j.carbpol.2021.118565.
Muthuraman, S., Flint, S., Palmer, J., 2025a. Characterization of the extracellular polymeric substances matrix of Pseudomonas biofilms formed at the air-liquid interface. Food Biosci. 64, 105918. https://doi.org/10.1016/j.fbio.2025.105918.
Muthuraman, S., Palmer, J., Flint, S., 2025b. Extracellular polymeric substances- the real target in eradicating pseudomonad biofilms. Food Biosci. 71, 107330. https://doi.org/10.1016/j.fbio.2025.107330.
Nahar, S., Mizan, M.F.R., Ha, A.J.W., Ha, S.D., 2018. Advances and future prospects of enzyme-based biofilm prevention approaches in the food industry. Compr. Rev. Food Sci. Food Saf. 17 (6), 1484–1502.
Nguyen, U.T., Burrows, L.L., 2014. DNase I and proteinase K impair Listeria monocytogenes biofilm formation and induce dispersal of pre-existing biofilms. Int. J. Food Microbiol. 187, 26–32. https://doi.org/10.1016/j.ijfoodmicro.2014.06.025.
Pant, K.J., Cotter, P.D., Wilkinson, M.G., Sheehan, J.J., 2023. Towards sustainable Cleaning-in-Place (CIP) in dairy processing: Exploring enzyme-based approaches to cleaning in the Cheese industry. Compr. Rev. Food Sci. Food Saf. 22, 3602–3619. https://doi.org/10.1111/1541-4337.13206.
Parkar, S.G., Flint, S.H., Brooks, J.D., 2004. Evaluation of the effect of cleaning regimes on biofilms of thermophilic bacilli on stainless steel. J. Appl. Microbiol. 96 (1), 110–116. https://doi.org/10.1046/j.1365-2672.2003.02136.x.
Parlapani, F.F., Anagnostopoulos, D.A., Karamani, E., Mallouchos, A., Haroutounian, S. A., Boziaris, I.S., 2023. Growth and volatile organic compound production of *Pseudomonas* fish spoiler strains on fish juice agar model substrate at different temperatures. Microorganisms 11 (1), 189. https://doi.org/10.3390/microorganisms11010189.
Puga, C.H., Rodríguez-López, P., Cabo, M.L., San Jose, C., Orgaz, B., 2018. Enzymatic dispersal of dual-species biofilms carrying Listeria monocytogenes and other associated food industry bacteria. Food Control 94, 222–228.
Raposo, A., Pérez, E., De Faria, C.T., Ferrús, M.A., Carrascosa, C., 2016. Food Spoilage by *Pseudomonas* spp.—An Overview. In: Singh, O.V. (Ed.), Foodborne Pathogens and Antibiotic Resistance, 1st ed. Wiley, pp. 41–71. https://doi.org/10.1002/9781119139188.ch3.
Rubio-Canalejas, A., Baelo, A., Herbera, S., Blanco-Cabra, N., Vukomanovic, M., Torrents, E., 2022. 3D spatial organization and improved antibiotic treatment of a Pseudomonas aeruginosa–Staphylococcus aureus wound biofilm by nanoparticle enzyme delivery. Front. Microbiol. 13, 959156. https://doi.org/10.3389/fmicb.2022.959156.
Sharma, K., Pagedar Singh, A., 2018. Antibiofilm Effect of DNase against Single and Mixed Species Biofilm. Foods 7 (3), 42. https://doi.org/10.3390/foods7030042.
Tang, X., Flint, S.H., Bennett, R.J., Brooks, J.D., 2010. The efficacy of different cleaners and sanitisers in cleaning biofilms on UF membranes used in the dairy industry. J. Membr. Sci. 352 (1–2), 71–75. https://doi.org/10.1016/j.memsci.2010.01.063.
Wang, D., Fletcher, G.C., Gagic, D., On, S.L.W., Palmer, J.S., Flint, S.H., 2023. Comparative genome identification of accessory genes associated with strong biofilm formation in Vibrio parahaemolyticus. Food Res. Int. 166, 112605. https://doi.org/10.1016/j.foodres.2023.112605.
Wang, S., Liu, X., Liu, H., Zhang, L., Guo, Y., Yu, S., Wozniak, D.J., Ma, L.Z., 2015. The exopolysaccharide Psl–eDNA interaction enables the formation of a biofilm skeleton in *P seudomonas aeruginosa*. Environ. Microbiol. Rep. 7 (2), 330–340. https://doi.org/10.1111/1758-2229.12252.
Wickramasinghe, N.N., Ravensdale, J.T., Coorey, R., Dykes, G.A., Scott Chandry, P., 2019. *In situ* characterisation of biofilms formed by psychrotrophic meat spoilage pseudomonads. Biofouling 35 (8), 840–855. https://doi.org/10.1080/08927014.2019.1669021.
Wiedmann, M., Weilmeier, D., Dineen, S.S., Ralyea, R., Boor, K.J., 2000. Molecular and phenotypic characterization of *Pseudomonas* spp. isolated from milk. Appl. Environ. Microbiol. 66 (5), 20852095. https://doi.org/10.1128/AEM.66.5.2085-2095.2000.
Xu, Z., Liang, Y., Lin, S., Chen, D., Li, B., Li, L., Deng, Y., 2016. Crystal Violet and XTT Assays on Staphylococcus aureus Biofilm Quantification. Curr. Microbiol 73, 474–482. https://doi.org/10.1007/s00284-016-1081-1.
Yuan, L., Sadiq, F.A., Wang, N., Yang, Z., He, G., 2021. Recent advances in understanding the control of disinfectant-resistant biofilms by hurdle technology in the food industry. Crit. Rev. Food Sci. Nutr. 61, 3876–3891. https://doi.org/10.1080/10408398.2020.1809345.
Zhao, J., Zhai, Z., Sun, D., Yang, C., Zhang, X., Huang, N., Jiang, X., Yang, K., 2019. Antibacterial durability and biocompatibility of antibacterial-passivated 316L stainless steel in simulated physiological environment. Materials Science Engineering C 100, 396–410. https://doi.org/10.1016/j.msec.2019.03.021.